Supplementary material for LHCb-PAPER-2015-013
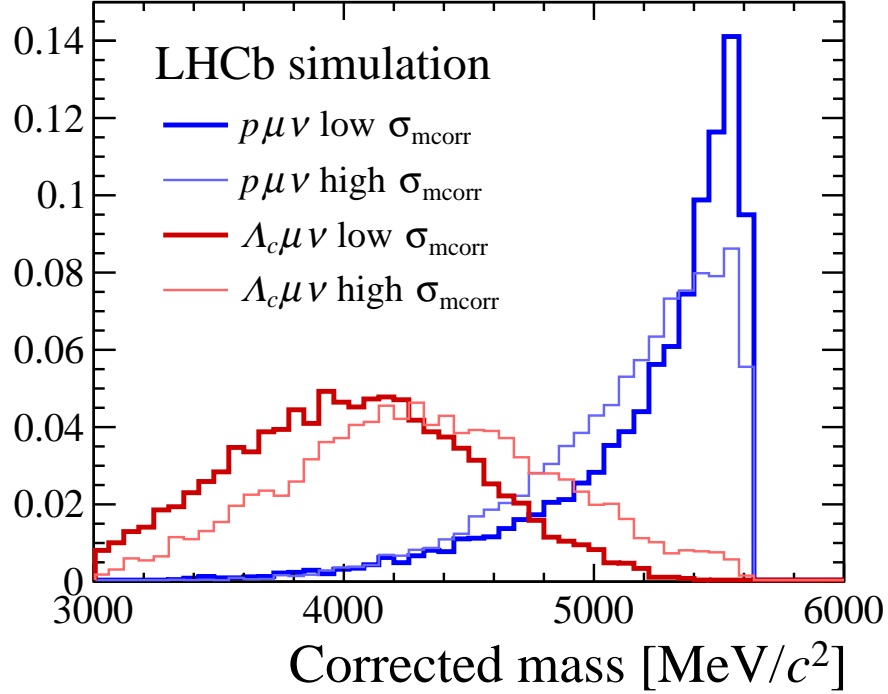

Figure 1: Distributions in m_{corr} of $\Lambda_b^0 \to p\mu^-\overline{\nu}_\mu$ and $\Lambda_b^0 \to \Lambda_c^+\mu^-\overline{\nu}_\mu$ candidates selected candidates in the simulation. In bold (thin) line for events with the estimated uncertainty in m_{corr} below $100\,\mathrm{MeV}/c^2$ (above $200\,\mathrm{MeV}/c^2$). It can be seen how the separation between the $\Lambda_b^0 \to p\mu^-\overline{\nu}_\mu$ signal and the $\Lambda_b^0 \to \Lambda_c^+\mu^-\overline{\nu}_\mu$ background improves dramatically by selecting events with low estimated uncertainty.
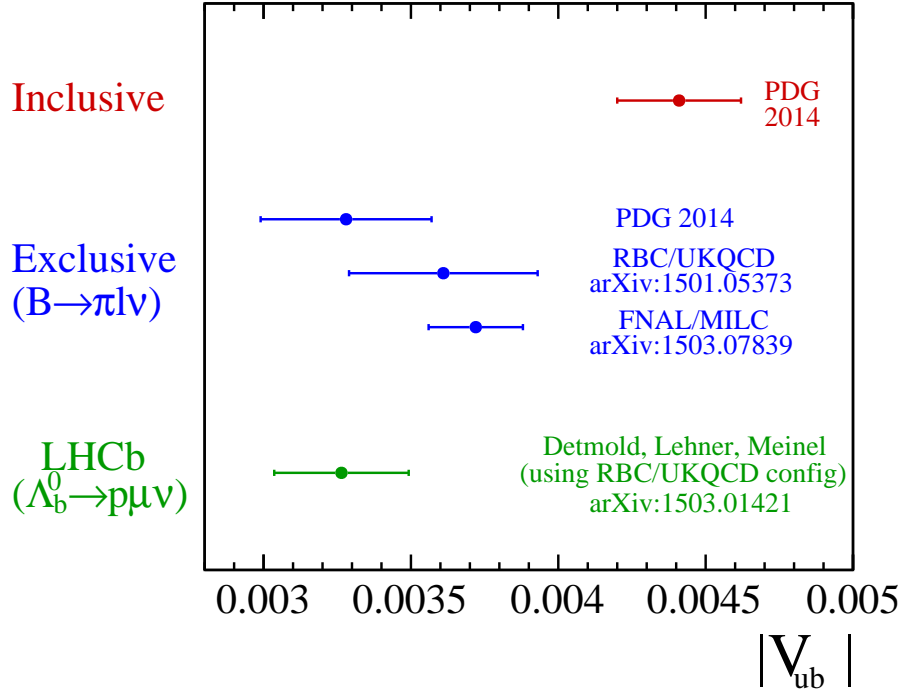
Figure 2: Comparison of the $|V_{ub}|$ result presented in the paper with the measurement obtained from inclusive decays and determinations using the exclusive decay $B \to \pi \ell \nu$.
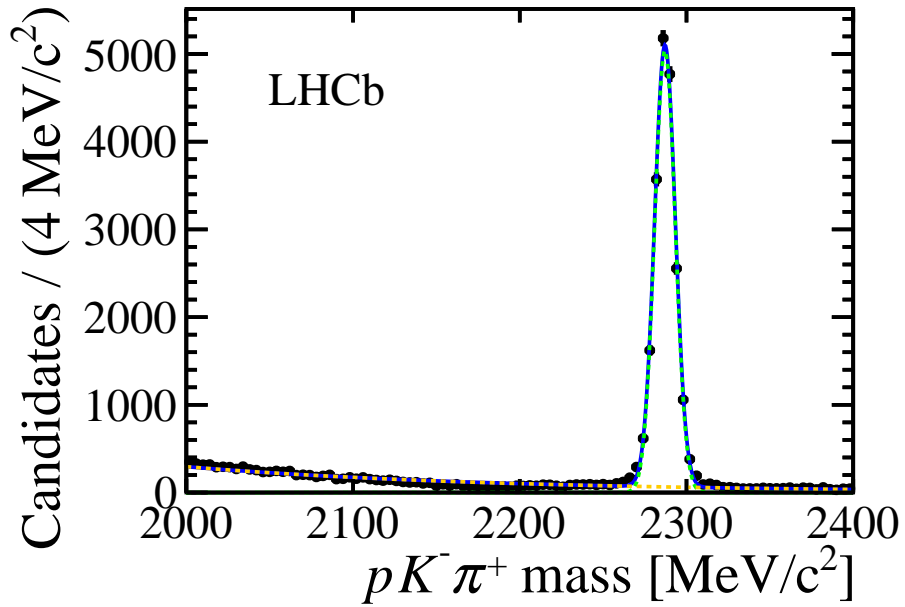

Figure 3: Mass fit to $\Lambda_b^0 \to (\Lambda_c^+ \to pK^-\pi^+)\mu^-\overline{\nu}_\mu$ candidates used to control the level of this background for the $\Lambda_b^0 \to p\mu^-\overline{\nu}_\mu$ signal fit.
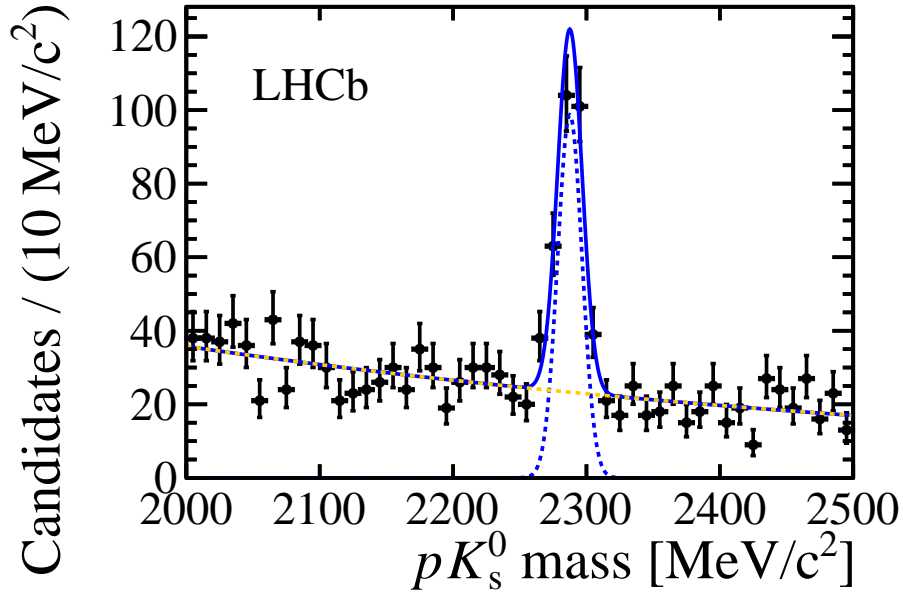
2

Figure 4: Mass fit to $\Lambda_b^0 \to (\Lambda_c^+ \to pK_S^0)\mu\nu$ candidates used to control the level of this background for the $\Lambda_b^0 \to p\mu^-\overline{\nu}_\mu$ signal fit.
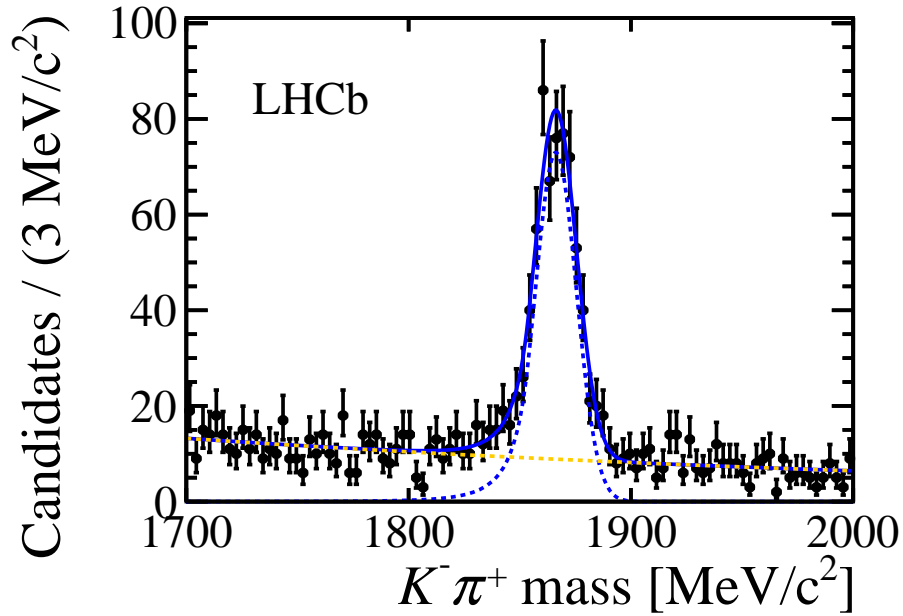

Figure 5: Mass fit to $\Lambda_b^0 \to (D^0 \to K^-\pi^+)p\mu\nu$ candidates used to control the level of this background for the $\Lambda_b^0 \to p\mu^-\overline{\nu}_\mu$ signal fit.
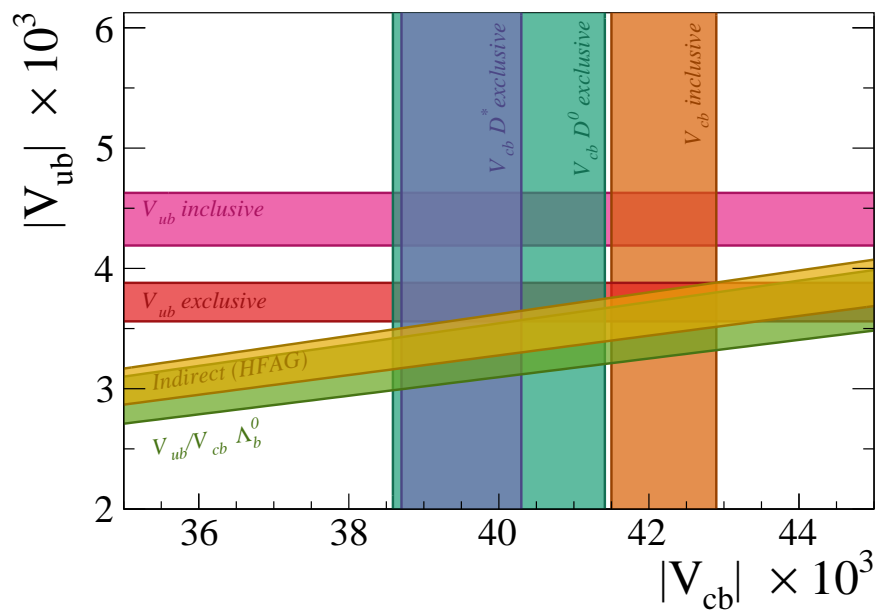
Figure 6: Two-dimensional plot, showing the constraints on $|V_{ub}|$ and $|V_{cb}|$. The existing $|V_{ub}|$ and $|V_{cb}|$ measurements are taken from the PDG 2015 update.